

The following resources related to this article are available online at www.sciencemag.org (this information is current as of September 18, 2009):

Updated information and services, including high-resolution figures, can be found in the online version of this article at:

<http://www.sciencemag.org/cgi/content/full/320/5877/778>

Supporting Online Material can be found at:

<http://www.sciencemag.org/cgi/content/full/1153360/DC1>

A list of selected additional articles on the Science Web sites **related to this article** can be found at:

<http://www.sciencemag.org/cgi/content/full/320/5877/778#related-content>

This article **cites 12 articles**, 2 of which can be accessed for free:

<http://www.sciencemag.org/cgi/content/full/320/5877/778#otherarticles>

This article has been **cited by** 16 article(s) on the ISI Web of Science.

This article has been **cited by** 3 articles hosted by HighWire Press; see:

<http://www.sciencemag.org/cgi/content/full/320/5877/778#otherarticles>

This article appears in the following **subject collections**:

Atmospheric Science

<http://www.sciencemag.org/cgi/collection/atmos>

Information about obtaining **reprints** of this article or about obtaining **permission to reproduce this article** in whole or in part can be found at:

<http://www.sciencemag.org/about/permissions.dtl>

The motion in these simulations can be markedly fast, up to about 10^8 $\mu\text{m/s}$. By comparison, the velocity of kinesin-propelled microtubules is typically about 1 $\mu\text{m/s}$, whereas actin mobility can reach speeds up to 10 $\mu\text{m/s}$ (31). However, the velocity that we observe experimentally is only up to about 1 $\mu\text{m/s}$ (21). The large difference in velocity between the experiments and simulations is attributed to the difference in the system dimensions. Considering that the number of atoms of the outer nanotube used in the experiments is about 100 times as large as the number of atoms of the nanotube used in the simulations, and taking Eq. 1 with typical values for the temperature and the barrier height (for example, 1300 K and 17 μeV per atom), we obtain a factor of about eight orders of magnitude difference for the velocity, which is consistent with the mismatch between the experiments and simulations. Because our calculation capabilities do not allow speeds down to 1 $\mu\text{m/s}$ to be reached, a direct comparison of the experiments and simulations cannot be made.

Although the temperature in our experiments may appear to be high, it should be possible to reduce it, which would be convenient for certain applications. To achieve this goal, researchers must make the dimensions of the movable nanotube narrower and shorter in order to reduce the barrier height. Another possible solution would be to selectively excite specific phonon modes, so that the average temperature of the phonon bath is lower. Indeed, not all of the phonon modes are expected to interact in the same way with the movable nanotube, and some are likely to be more effective in transferring momentum, such as the breathing modes.

The actuation by means of thermal gradients has obvious potential for NEMS applications. Thermal gradients could be used to drive the flow of fluids inside nanotubes or in nanofluidic devices or used for drug delivery by nanosyringes. The thermal gradient actuation may also be applied to bioengineered nanopores via, for example, the heat generated from the hydrolysis of adenosine triphosphate molecules. Using methods to align nanotubes on substrates, researchers should be able to fabricate arrays of orientationally ordered nanotube-based thermal motors.

References and Notes

- M. L. Roukes, *Phys. World* **14**, 25 (2001).
- V. V. Deshpande *et al.*, *Nano Lett.* **6**, 1092 (2006).
- A. M. Fennimore *et al.*, *Nature* **424**, 408 (2003).
- B. Bourlon, D. C. Glattli, C. Miko, L. Forro, A. Bachtold, *Nano Lett.* **4**, 709 (2004).
- B. C. Regan, S. Aloni, R. O. Ritchie, U. Dahmen, A. Zettl, *Nature* **428**, 924 (2004).
- K. Svensson, H. Olin, E. Olsson, *Phys. Rev. Lett.* **93**, 145901 (2004).
- D. Golberg *et al.*, *Adv. Mater.* **19**, 1937 (2007).
- R. Saito, R. Matsuo, T. Kimura, G. Dresselhaus, M. S. Dresselhaus, *Chem. Phys. Lett.* **348**, 187 (2001).
- Yu. E. Lozovik, A. V. Belikov, A. M. Popov, *Phys. Lett. A* **313**, 112 (2003).
- P. A. E. Schoen, J. H. Walther, S. Arcidiacono, D. Poulikakos, P. Koumoutsakos, *Nano Lett.* **6**, 1910 (2006).
- P. A. E. Schoen, J. H. Walther, D. Poulikakos, P. Koumoutsakos, *Appl. Phys. Lett.* **90**, 253116 (2007).
- Z. C. Tu, X. Hu, *Phys. Rev. B* **72**, 033404 (2005).
- R. D. Astumian, P. Hanggi, *Phys. Today* **55**, 33 (2002).
- A. N. Kolmogorov, V. H. Crespi, *Phys. Rev. Lett.* **85**, 4727 (2000).
- P. Tangney, M. L. Cohen, S. G. Louie, *Phys. Rev. Lett.* **97**, 195901 (2006).
- J. Servantie, P. Gaspard, *Phys. Rev. B* **73**, 125428 (2006).
- P. G. Collins, M. S. Arnold, Ph. Avouris, *Science* **292**, 706 (2001).
- P. G. Collins, M. Hersam, M. Arnold, R. Martel, Ph. Avouris, *Phys. Rev. Lett.* **86**, 3128 (2001).
- B. Bourlon *et al.*, *Phys. Rev. Lett.* **92**, 026804 (2004).
- Most of the low-resistive devices engineered with the electrical-breakdown technique can be actuated with an electron current, although this is never the case for the non-engineered devices (21).
- Materials and methods are available as supporting material on Science Online.
- M. F. Yu, B. I. Yakobson, R. S. Ruoff, *J. Phys. Chem. B* **104**, 8764 (2000).
- A. Kis, K. Jensen, S. Aloni, W. Mickelson, A. Zettl, *Phys. Rev. Lett.* **97**, 025501 (2006).
- E. R. Kay, D. A. Leigh, F. Zerbetto, *Angew. Chem. Int. Ed.* **46**, 72 (2007).
- S. Chen *et al.*, *Appl. Phys. Lett.* **87**, 263107 (2005).
- G. S. Kottas, L. I. Clarke, D. Horinek, J. Michl, *Chem. Rev.* **105**, 1281 (2005).
- G. E. Begtrup *et al.*, *Phys. Rev. Lett.* **99**, 155901 (2007).
- We do not observe any change of the electron resistance when comparing samples with and without gold cargoes. As a result, we do not expect a substantial modification of the spatial temperature profile in these two configurations. A direct consequence of this temperature profile is that the speed of the cargo is not constant along the nanotube. It is highest near the midpoint of the tube and lowest near the contacts (fig. S2).
- The temperature profile is likely to be slightly asymmetric with respect to the middle of the nanotube resulting from, for example, different contact resistances. As a result, the mobile element can move even if it is placed exactly in the middle of the nanotube.
- J. Tersoff, *Phys. Rev. Lett.* **61**, 2879 (1988).
- M. G. L. van den Heuvel, C. Dekker, *Science* **317**, 333 (2007).
- We thank J. Llobet, G. Rius, and X. Borrísé for valuable help with the experiments, as well as P. Ordejon and M. Monthieux for discussions. Financial support from a European Young Investigator grant, the European Union-funded project FP6-IST-021285-2, the grants FIS2006-12117-C04 and TEC2006-13731-C02-01 from the Ministerio de Educación y Ciencia, a Ramón y Cajal Fellowship, and the grant 2005SGR683 from Agència de Gestió d'Ajuts Universitaris i de Recerca is acknowledged. The work in Lausanne was supported by the Swiss NSF and its National Centres of Competence in Research "Nanoscale Science."

Supporting Online Material

www.sciencemag.org/cgi/content/full/1155559/DC1

Materials and Methods

Figs. S1 to S5

Tables S1 and S2

References

Movies S1 to S5

22 January 2008; accepted 31 March 2008

Published online 10 April 2008;

10.1126/science.1155559

Include this information when citing this paper.

Fracture Propagation to the Base of the Greenland Ice Sheet During Supraglacial Lake Drainage

Sarah B. Das,^{1*} Ian Joughin,² Mark D. Behn,¹ Ian M. Howat,^{2,3} Matt A. King,⁴ Dan Lizarralde,¹ Maya P. Bhatia⁵

Surface meltwater that reaches the base of an ice sheet creates a mechanism for the rapid response of ice flow to climate change. The process whereby such a pathway is created through thick, cold ice has not, however, been previously observed. We describe the rapid (<2 hours) drainage of a large supraglacial lake down 980 meters through to the bed of the Greenland Ice Sheet initiated by water-driven fracture propagation evolving into moulin flow. Drainage coincided with increased seismicity, transient acceleration, ice-sheet uplift, and horizontal displacement. Subsidence and deceleration occurred over the subsequent 24 hours. The short-lived dynamic response suggests that an efficient drainage system dispersed the meltwater subglacially. The integrated effect of multiple lake drainages could explain the observed net regional summer ice speedup.

The Greenland Ice Sheet flows outward from its interior through a combination of internal deformation and basal sliding, losing mass around its edges through meltwater runoff and iceberg calving. Recent observations show that ice flow along the western margin accelerates during the summer when surface meltwater lubricates sliding at the ice-bedrock interface (1, 2). Aside from theoretical predictions (3–5) and observations on small icecaps (6), it has not been established how surface meltwater penetrates through thick, subfreezing ice (7, 8). Ice-sheet

models used to predict future sea-level rise typically do not include the impact of surface meltwater on ice dynamics. Attempts to include the effects of enhanced basal lubrication within these models suggest that increased meltwater may substantially accelerate ice-sheet mass loss, but confidence in these results is limited by a poor understanding of ice-sheet hydrology (9). Key unknowns in determining Greenland's potential response to climate forcing are the time scales and pathways through which meltwater reaches the ice sheet's base and its consequent effect on basal motion (10).

For surface meltwater to reach the ice-sheet bed, a through-ice conduit is required. Theoretical models of fracture propagation through ice suggest that once initiated, water-filled crevasses will propagate rapidly downward through the full ice thickness to the bed (3–5). In such models, the rate of crack propagation is limited only by the meltwater supply needed to keep the crack full (3, 4). Supraglacial lakes (11–13) can provide the large volumes of water required to propagate fractures to the bed (7); thus, these lakes are likely critical for establishing a through-ice conduit (moulin). Furthermore, moulins that form in lake basins lie near the confluence of meltwater streams and will continue to be supplied with surface meltwater after the lake drains, routing water to the bed and delaying closure while sufficient meltwater production continues throughout the summer.

To investigate lake drainage and the ensuing ice-sheet response, we established study sites at two large (~2-km diameter) lakes on the ice sheet's western margin at locations with thick (~980 m) (14), subfreezing ice (15). During July 2006, our northernmost study lake (68.72°N, -49.50°W) drained rapidly in an event captured by local Global Positioning System (GPS), seismic, and water-level sensors (Fig. 1) (16). A similar, although less well documented, drainage event occurred at this lake again in 2007 (fig. S1).

The lake began filling in early July 2006, reaching its maximum extent around 00:00 (UTC) on 29 July 2006, with a surface area of 5.6 km² and a volume of 0.044 ± 0.01 km³ (16). The lake level then began to fall slowly and steadily at 1.5 cm/hour. At ~16:00 UTC the same day, the lake level began dropping rapidly, reaching a maximum drop rate of 12 m/hour between 16:40 and 17:00 (Fig. 2). Extrapolation of the depth-logger data (Fig. 2) indicates that the entire lake drained in ~1.4 hours. The average drainage rate (8700 m³/s) during this rapid-drainage phase exceeded the average flow rate over Niagara Falls.

Local vertical and horizontal movement of the ice sheet occurred coincident with the lake drainage. A GPS station located ~0.5 km north of the lake (Fig. 1) recorded both rapid uplift (1.2 m) and northward horizontal motion (0.8 m), with the maximum surface displacement occurring between 17:15 and 17:30 UTC (Fig. 2). This northward motion was substantially faster and orthogonal to the mean westerly velocity of 93 m/year. The following 24-hour period was

characterized by gradual subsidence and return to the mean westerly motion accompanied by a transient speedup in the downflow direction. In total, the event resulted in a net westerly surface displacement of 0.5 m in excess of the average daily displacement of 0.25 m (Fig. 2C and fig. S2.)

A seismometer located ~0.7 km north of the lake (Fig. 1) recorded elevated activity beginning around 15:30 UTC, ~30 min before the period of rapid lake drainage. The maximum amplitude in seismic energy occurred between 16:45 and 18:00 UTC, during and slightly after the period of rapid lake drainage (fig. S3).

Site visits provided observations of pre-drainage (July 2006) and post-drainage (July 2007) surface features. We found several km-scale fractures running through the lake basin in 2007. Many were closed at depth (water filled) and no longer draining. Two large moulins were found along the fractures, actively draining the area in 2007 (Fig. 1). A dominant topographic feature in 2007 was an uplifted section of the ice sheet roughly centered over the lake bottom, forming a

flat-topped block of ice ~6 m high and 750 m wide (Fig. 1). This block likely was uplifted as water was rapidly injected to the base of the ice sheet near the lake's center during the 2006 drainage event (16). The block's southern edge lay along a ~3.2-km fracture visible from the air and in synthetic aperture radar (SAR) imagery spanning the lake basin's full width; the northern edge lay along a similarly visible fracture (Fig. 1).

The observed fractures and rapid drainage, synchronous with uplift and horizontal acceleration, are strong evidence that water-driven fracture propagation likely established a hydrological connection to the bed. These observations suggest that hydrologic connectivity occurs in four stages: slow initial drainage; connection to the bed and rapid lake drainage through an extensive fracture system; moulin formation and closure of fractures; and subsequent moulin-routed drainage of daily surface meltwater to the ice-sheet bed.

The 16-hour initial drainage stage was characterized by a slow, steady drop in lake level, elevated seismicity in the 30 min before rapid

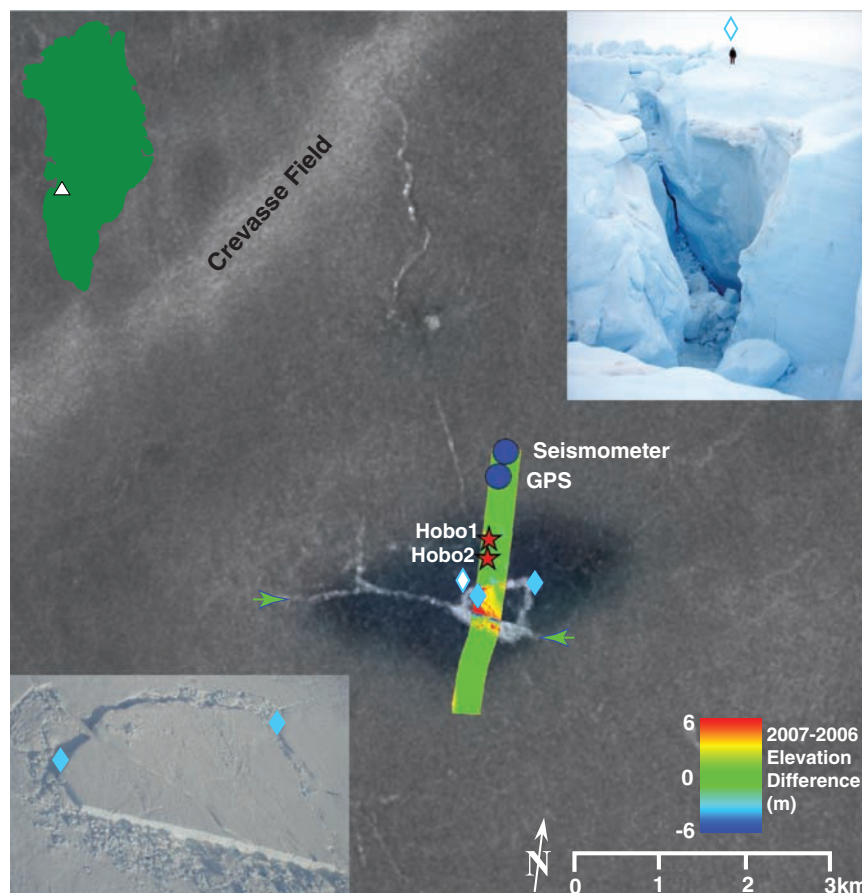


Fig. 1. Early October 2006 SAR image (gray-scale background) overlaid with a semi-transparent image recorded by NASA's Moderate Resolution Imaging Spectroradiometer (MODIS) showing the lake extent (blue) on 29 July 2006. Red stars show the water-pressure logger locations and blue circles show the GPS/seismometer locations. Block uplift (lower-left inset) is revealed by 2006 to 2007 elevation differences (colored swath) recorded by NASA's Airborne Topographic Mapper (ATM) in May of both years. A large fracture is visible in the SAR image as a long, bright linear feature with ends marked by green arrows. Solid blue diamonds indicate locations where sonar and ATM measurements found large "holes" in the lake bed before drainage in 2006. The upper-right inset shows a 1.8-m-tall person standing above a similar hole (open blue diamond) located after the 2007 lake drainage.

¹Department of Geology and Geophysics, Woods Hole Oceanographic Institution, Woods Hole, MA 02543, USA.

²Polar Science Center, Applied Physics Lab, University of Washington, 1013 NE 40th Street, Seattle, WA 98105-6698, USA. ³School of Earth Sciences and Byrd Polar Research Center, The Ohio State University, 1090 Carmack Road, Columbus, OH 43210-1002, USA. ⁴School of Civil Engineering and Geosciences, Newcastle University, Newcastle upon Tyne, NE1 7RU, UK. ⁵Department of Geology and Geophysics, Massachusetts Institute of Technology/Woods Hole Oceanographic Institution Joint Program, Woods Hole, MA 02543, USA.

*To whom correspondence should be addressed. E-mail: sdas@whoi.edu

drainage (fig. S3), and little or no acceleration or uplift at the GPS site (Fig. 2). This initial phase may have coincided with water-filled fracture propagation beneath the lake through the kilometer-thick ice. The main crack's 3.2-km length (Fig. 1) could have stored a volume of water corresponding to the initial lake-level drop, assuming a 0.5-m-wide average opening. Alternatively, the predrainage may have started as the lake began spilling over a low drainage divide where the main fracture intersects the western shoreline, filling an existing dry crack at the lake edge so that it hydro-fractured into and through the ice beneath the lake. Surface strain rates from satellite derived-velocities (I) are tensile ($\epsilon_{xx} = 0.003 \text{ year}^{-1}$; x directed along flow) along this western shoreline, favoring crevasse formation, whereas strain rates near the lake's center are compressive ($\epsilon_{xx} = -0.004 \text{ year}^{-1}$). At neighboring lakes, we observed similar situations in which lakes spilled over into shoreline cracks, creating moulins. Where the fracturing ran adjacent to rather than through the lake basin, drainage occurred over weeks as overflow melted and deepened the spillover channel leading to the moulin. For either hypothesis, the low seismicity, lack of uplift and acceleration, and the slow drainage rate suggest that little or no water reached the bed of the ice sheet during this first stage.

The second stage began when the fractures breached the full ice thickness, establishing a direct connection to the basal hydrological system. Rapid lake drainage (1.4 hours) was accompanied by an increase in seismic energy (fig. S3) and synchronous surface displacement of the adjacent shoreline up (1.2 m) and away (0.8 m) from the lake center (Fig. 2). The short duration between the drop in lake level and shore-based surface motion indicates rapid and direct transport of water to the bed. Uplift at the center of the lake was likely larger than the 1.2 m observed nearby on shore, and probably coincided with uplift of the large block at the lake's center. The synchronous uplift indicates a nearly vertical path to the bed, as well as the formation of a transient subglacial lake that displaced the overlying ice. The high drainage rate and the presence of rafted ice blocks observed along lake-bed fractures suggest that drainage occurred along most of the fractures' length. The turbulent water flow during the rapid discharge would have melted the fracture walls through frictional heating, concentrating flow paths and leading to the development of larger-diameter openings at points where inflow was greatest (6).

We hypothesize that during the third stage, which lasted a few days after the rapid lake drainage, most of the fractures closed at depth and discrete moulins formed. The surface water flow (~24 m³/s) previously filling the lake provided inflow into the areas still connected to the bed. Melt widening at locations where inflow was greatest (e.g., at the ends of surface streams), competing with the tendency of overburden pressure to close the no-longer water-filled fractures,

probably produced and maintained a few discrete moulins that remained open throughout the remainder of the melt season (fourth stage), similar to those we observed after drainage in 2007 (Fig. 1).

Also during the third stage, the transient subglacial lake drained over a ~24-hour period, as suggested by the GPS-measured vertical subsidence and horizontal southward motion (Fig. 2 and fig. S2). The relatively rapid subglacial lake drainage suggests the presence of an efficient subglacial hydrological system. Increased ice fracturing likely occurred during this stage as well, possibly explaining the elevated seismic energy in the 1-hour period immediately following the lake drainage (fig. S3).

Throughout the melt season, the onshore GPS recorded fluctuations in ice-sheet velocity of 50 to 100% that correlate well with calculations of daily melt intensity and regional ice-sheet flow (I). Other than the ~24-hour period following the drainage (Fig. 2 and fig. S2), the character of the pre- and postdrainage speed fluctuations did not differ appreciably (I). Thus, the opening of a new moulin draining a large daily melt volume (24 m³/s) had little apparent lasting effect on the local ice-sheet velocity. Instead, we hypothesize that this event contributed to the collective formation of a network of regionally distributed moulins supplying meltwater to the bed that modulated ice flow both before and after the drainage event. Such modulation implies the presence of a well-connected subglacial drainage system capable of receiving water inflow at discrete locations

and dispersing it uniformly beneath the ice sheet. This creates what appears to be partial ice-bed decoupling associated with a distributed subglacial hydrological system. These indirect observations highlight how much remains to be learned about the subglacial environment beneath the Greenland Ice Sheet.

Our lake-drainage observations provide evidence for a fracture-driven process opening a 1-km-deep through-ice conduit and injecting a large volume of surface meltwater directly beneath the ice sheet. Although fracturing established the initial connection, additional melting from energy dissipation during the turbulent flow of water in its 1-km descent likely played a role in widening and maintaining discrete moulins that stayed open throughout the remainder of the melt season. Thousands of lakes are formed on the ice sheet's surface throughout the ablation season, and although we have detailed observations from only a single lake, we do not believe the lake drainage we observed was an isolated or unique event. Other Greenland supraglacial lakes have previously been observed to disappear from the surface in 1 day (12). During ground and aerial surveys in 2006 and 2007, we investigated more than 10 surrounding lake basins near our study site and detected numerous streams draining into moulins across the ice sheet's surface. These systems were observed both where lakes had drained completely and also where lakes cut overflow channels that later drained into nearby fractures and moulins. In addition, all of the postdrainage lake basins that we observed had fractures running

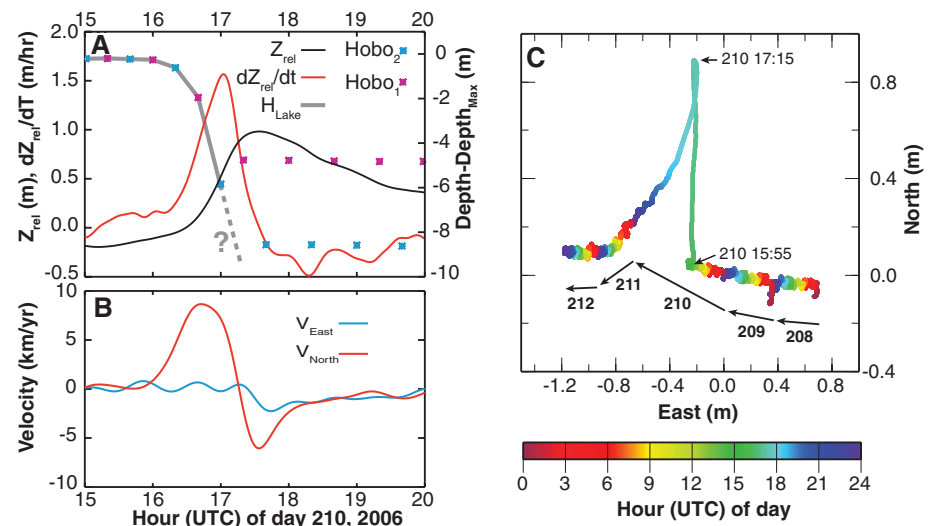


Fig. 2. Data from the 2006 lake drainage event. **(A)** Relative elevation (z_{rel}) and rate of elevation change (left axis: black and red lines respectively) are derived from the on-shore GPS elevations smoothed to 5-min temporal resolution. Lake level as recorded by water-pressure loggers (right axis: blue and magenta stars connected with a gray line) and referenced to the lake level just before drainage. A linear fit to the last two lake-level measurements when the depth loggers remained submerged suggests that the lake drained completely by ~17:30 UTC (dashed gray line). **(B)** North (red) and east (blue) velocity components at the GPS station smoothed to 10-min temporal resolution. **(C)** Relative position of the GPS station during the 5 days before, during, and after the drainage event showing the rapid translation of the surface as it floats up and away from the lake center, and subsequently returns. The color-bar indicates the hour of day, and the bold black arrows delineate each day's net motion.

across their surface, supporting the fracture-based mechanism for rapid drainage that we have described for our study lake.

Thus, we have shown that water-driven fracture enabled by the large volume of water stored in supraglacial lakes provides a means by which hydrologic surface-to-bed connections are established through thick ice. Climate warming would lead to earlier and expanded surface lake formation and, as a result, connections to the bed may occur earlier in the melt season and over a larger area, although further work is needed to constrain the limits of this area. This would increase the annual subglacial throughput of meltwater and may substantially impact Greenland Ice Sheet dynamics (1).

References and Notes

1. I. Joughin *et al.*, *Science* **320**, 781 (2008); published online 17 April 2008 (10.1126/science.1153288).
2. H. J. Zwally *et al.*, *Science* **297**, 218 (2002).

3. C. J. van der Veen, *Geophys. Res. Lett.* **34**, L01501 (2007).
4. R. B. Alley, T. K. Dupont, B. R. Parizek, S. Anandakrishnan, *Ann. Glaciol.* **40** (2005).
5. J. Weertman, in *Symposium on the Hydrology of Glaciers*, Cambridge, 7 to 13 September 1969 (International Association of Hydrologic Sciences, Cambridge, 1973), pp. 139–145.
6. S. Boon, M. Sharp, *Geophys. Res. Lett.* **30**, 1916 (2003).
7. J. L. Bamber, R. B. Alley, I. Joughin, *Earth Planet. Sci. Lett.* **257**, 1 (2007).
8. S. J. Marshall, *Earth Planet. Sci. Lett.* **240**, 191 (2005).
9. B. R. Parizek, R. B. Alley, *Quat. Sci. Rev.* **23**, 1013 (2004).
10. IPCC, *Climate Change 2007: The Physical Science Basis. Contribution of Working Group I to the Fourth Assessment Report of the Intergovernmental Panel on Climate Change* (Cambridge Univ. Press, Cambridge and New York, 2007).
11. M. McMillan, P. Nienow, A. Shepherd, T. Benham, A. Sole, *Earth Planet. Sci. Lett.* **262**, 484 (2007).
12. J. E. Box, K. Ski, *J. Glaciol.* **53**, 257 (2007).
13. M. Luthje, L. T. Pedersen, N. Reeh, W. Greuell, *J. Glaciol.* **52**, 608 (2006).
14. S. Gogineni *et al.*, *J. Geophys. Res.* **106**, 33761 (2001).
15. R. Greve, *J. Clim.* **10**, 901 (1997).

16. Methods are available as supporting material on *Science* Online.
17. Support was provided jointly by NSF and NASA through ARC-0520077 (S.B.D., M.P.B., I.M.H.) and ARC-520382 (I.J.). The Woods Hole Oceanographic Institution Ocean and Climate Change Institute and Clark Arctic Research Initiative provided additional support to S.B.D., M.D.B., and D.L.; and a Natural Environment Research Council (UK) Research Fellowship supported M.A.K. Logistical and instrumental support was provided by VECO Polar Resources, PASSCAL, and UNAVCO. Early conversations with R.B. Alley helped initiate this project. Comments from two anonymous reviewers substantially improved the content and clarity of the manuscript. The ATM data were kindly provided by B. Krabill and S. Manizade.

Supporting Online Material

www.sciencemag.org/cgi/content/full/1153360/DC1

Methods

Figs. S1 to S3

References

26 November 2007; accepted 31 March 2008

Published online 17 April 2008;

10.1126/science.1153360

Include this information when citing this paper.

Seasonal Speedup Along the Western Flank of the Greenland Ice Sheet

Ian Joughin,^{1*} Sarah B. Das,² Matt A. King,³ Ben E. Smith,¹ Ian M. Howat,^{1†} Twila Moon¹

It has been widely hypothesized that a warmer climate in Greenland would increase the volume of lubricating surface meltwater reaching the ice-bedrock interface, accelerating ice flow and increasing mass loss. We have assembled a data set that provides a synoptic-scale view, spanning ice-sheet to outlet-glacier flow, with which to evaluate this hypothesis. On the ice sheet, these data reveal summer speedups (50 to 100%) consistent with, but somewhat larger than, earlier observations. The relative speedup of outlet glaciers, however, is far smaller (<15%). Furthermore, the dominant seasonal influence on Jakobshavn Isbrae's flow is the calving front's annual advance and retreat. With other effects producing outlet-glacier speedups an order of magnitude larger, seasonal melt's influence on ice flow is likely confined to those regions dominated by ice-sheet flow.

Along its western margin, the Greenland Ice Sheet melts at rates that can exceed 2.5 m/year (1) as ice flows seaward at speeds of roughly 100 m/year. Embedded within the ice sheet are faster-flowing (200 to 12,000 m/year) outlet glaciers that discharge ice directly to the ocean. When the combined loss from melt and ice discharge, which now act in roughly equal proportions, removes more ice than is replaced by annual snowfall, the excess ice lost to the ocean contributes to sea-level rise.

Glacial motion results from a combination of internal deformation of ice under its own weight, sliding at the ice-bed interface, and deformation of underlying sediments. Basal sliding over a well-lubricated bed is often the source of fast (e.g., >100 m/year) ice motion (2). Seasonal fluctuation

in the drainage of rainfall and surface meltwater to the bed modulates the sliding speed of many alpine glaciers (3–5). Greenland's large coastal melt rates have prompted widespread speculation both in the popular media (6) and in the scientific literature (7, 8) that a warmer climate will increase melting, which in turn will enhance basal lubrication and hasten ice-sheet retreat. Poor knowledge of this process is one of the limitations on prediction of future ice-sheet contributions to sea-level rise that was noted by the Intergovernmental Panel on Climate Change (9).

The few studies of seasonal speedup in Greenland are equivocal about the importance of this lubrication effect. An early study of western Greenland's largest outlet glacier, Jakobshavn Isbrae, found no measurable seasonal speedup (10). One outlet glacier in northern Greenland, however, did undergo a short-term speedup, apparently in response to the drainage of a supraglacial lake (11). On the slow-moving ice sheet at Swiss Camp (Fig. 1), located just north of Jakobshavn Isbrae, a time series of Global Positioning System (GPS) observations showed seasonal speedups of 5 to 28% that correlated well with summer melt rates (7).

To better determine the influence of surface melting on ice-sheet flow, we have assembled a

comprehensive set of interferometric synthetic aperture radar (InSAR) and GPS observations (12). These data include 71 (September 2004 to August 2007) InSAR velocity maps along two partially overlapping RADARSAT tracks that include Jakobshavn Isbrae, several smaller marine-terminating outlet glaciers, and a several-hundred-kilometer-long stretch of the surrounding ice sheet. We also collected GPS observations from July 2006 to July 2007 at sites near two supraglacial lakes (Fig. 1) south of Jakobshavn Isbrae.

Figure 1 shows the August 2006 speedup measured with InSAR speckle tracking. Although there are coverage gaps, the data show a relatively uniform speedup extending over the bare-ice zone. To simplify the analysis, we used a 150-m/year threshold to partition the area into slower-moving "ice-sheet" and faster-moving "outlet-glacier" regions. Under this rough classification, the ice sheet sped up by 36 m/year (48%) above its 76-m/year mean speed, demonstrating increases over a broad area that are substantially larger than measured earlier at Swiss Camp (28%) (7). On the outlet glaciers, the 51-m/year speedup was larger, but this was only 8.6% faster than the 594-m/year mean. Although the InSAR coverage (not shown) is less complete, mid-July 2006 speedups were 71 (97%) and 77 m/year (14%) for the ice-sheet and outlet-glacier regions, respectively. Similar speedups occurred in summer 2007 (e.g., fig. S1).

Although RADARSAT provides good spatial coverage, its temporal resolution (24 days) is limiting. Two-day temporal resolution is available with GPS observations (Fig. 2) from two locations (North Lake and South Lake, Fig. 1). These data reveal periods of generally higher speeds (~50%) during two melt seasons, punctuated by several additional short-term speedups (~100%). The minimum velocity occurs with the late-summer cessation of melt, and speed then slowly increases through the winter before the late-spring large melt-induced speedup.

The GPS sites at both lakes show similar short- and long-term variation in speed, consistent with

¹Polar Science Center, Applied Physics Lab, University of Washington, 1013 NE 40th Street, Seattle, WA 98105–6698, USA. ²Department of Geology and Geophysics, Woods Hole Oceanographic Institution, Woods Hole, MA 02543, USA. ³School of Civil Engineering and Geosciences, Newcastle University, Newcastle upon Tyne NE1 7RU, UK.

*To whom correspondence should be addressed. E-mail: ian@apl.washington.edu

†Present address: The Ohio State University, 1090 Carmack Road, Columbus, OH 43210–1002, USA.